



## How a neuron model can demonstrate co-existence of tonic spiking and bursting

Gennady S. Cymbalyuk<sup>a,\*</sup>, Ronald L. Calabrese<sup>b</sup>,  
Andrey L. Shilnikov<sup>c</sup>

<sup>a</sup>*Department of Physics and Astronomy, Georgia State University, 29 Peachtree Center Av,  
Science Annex, Suite 400, Atlanta, GA 30303, USA*

<sup>b</sup>*Department of Biology, Emory University, Atlanta, GA 30322, USA*

<sup>c</sup>*Department of Mathematics and Statistics, Georgia State University, Atlanta, GA 30303, USA*

Available online 30 December 2004

---

### Abstract

Tonically spiking as well as bursting neurons are frequently observed in electrophysiological experiments. The theory of slow–fast dynamical systems can describe basic scenarios of how these regimes of activity can be generated and transitions between them can be made. Here, we suggest a biophysically plausible mechanism based on homoclinic bifurcations of a saddle periodic orbit which explains a transition between tonic spiking behavior and bursting behavior in a neuron model of Hodgkin–Huxley type. Also, this mechanism is featured by the coexistence of tonic spiking and bursting oscillations.

© 2004 Elsevier B.V. All rights reserved.

*Keywords:* Bi-stability; Bifurcations; Medicinal leech; Saddle orbits; Homoclinics

---

Neurons are observed in one of the three fundamental, broadly defined modes: silence, tonic spiking and bursting. The functional role of bursting has been actively discussed in recent theoretical and experimental studies. There is agreement that it is an important mode for control of rhythmic movements and is frequently observed in central pattern generators, neuronal networks controlling motor behavior [11]. Also,

---

\*Corresponding author. Tel.: 404 651 2841.

*E-mail address:* [gcym@phy-astr.gsu.edu](mailto:gcym@phy-astr.gsu.edu) (G.S. Cymbalyuk).

bursting has been widely observed in sleep and pathological brain states [20]. More recently, bursting has begun to be identified with other functions. It has been proposed to improve reliability of memory formation [9]. The coexistence of a tonic spiking mode and of different bursting modes with each other has been observed in modeling [2,3,5] and experimental [7,8,22] studies and this complexity adds potential flexibility to the nervous system. Such multistability may be controlled by neuromodulators and thus reflect the functional state of the nervous system. Multistability has many potential implications for dynamical memory and information processing in a neuron [3,22,12]. A mathematical model of a single neuron may demonstrate similar regimes, and variations of certain biophysical parameters in the model can cause transitions between these regimes. These regimes co-exist in certain parameter ranges depending on initial conditions or perturbation. Bursting behavior is well described and has been classified within a framework of the methods of qualitative theory of slow–fast systems [15]. Of special interest, here are various mechanisms for chaotic bursting analyzed in detail in [21,23], which occur in transitions from the regime of continuous spikes to bursting. Two other mechanisms of transition based on the blue-sky catastrophe [18] and saddle-node periodic orbit with noncentral homoclinics [10] are reported in [16,17]. Here, we report in detail a case in which the bifurcation behind the transition from tonic spiking into bursting is based on homoclinic bifurcations of a saddle periodic orbit. We refer to identified oscillator interneurons that are part of the leech heartbeat central pattern generator. When isolated pharmacologically from the rest of the network, these neurons show autonomous bursting behavior [5]. In these neurons, eight voltage-dependent ionic currents have been identified and characterized, see [6] and references therein. Classified by their ionic specificity, these currents are two sodium currents, a fast sodium current ( $I_{Na}$ ) and a persistent sodium current ( $I_{NaP}$ ); three potassium currents, a delayed rectifier-like potassium current ( $I_{K1}$ ), a persistent potassium current ( $I_{K2}$ ) and a fast transient potassium ( $I_{KA}$ ); two low-threshold calcium currents, one rapidly ( $I_{CaF}$ ) and one slowly inactivating ( $I_{CaS}$ ) and a hyperpolarization-activated current ( $I_h$ ). A canonical model of a single neuron has been constructed and tuned to reproduce experimentally observed behaviors [5,6]. As alluded above, a comprehensive analysis of this model would be quite difficult. Blockade of groups of currents in living heart interneurons simplifies neuronal dynamics, and elicit characteristic behaviors, like that observed under blockade of  $Ca^{2+}$  currents. In leech neurons, application of divalent ions like  $Co^{2+}$ , which block  $Ca^{2+}$  currents, along with partial block of outward currents, elicit slow plateau-like oscillations with up to 60s period and up to 20s plateau duration [1,13]. This phenomenon persists after a blockade of  $I_h$  [13].

Previously, in our modeling studies [4], we derived a simplified neuron model taking into account that the experimental conditions eliminated or reduced the contribution of certain currents into the dynamics of the neuron. To bring the canonical model developed in [6], in accordance with the experimental conditions described above, we remove from the model the equations and terms describing blocked currents:  $I_{CaF}$ ,  $I_{CaS}$ , and  $I_h$ . For simplicity, we assume that the partial block of outward currents completely removes  $I_{K1}$  and  $I_{KA}$ , whereas it reduces  $I_{K2}$ . The current  $I_{NaP}$  is removed for simplicity. Here, we employ the model described in [4] with the parameter values taken from [16] (for the equations, see Appendix). In terms

of dynamical systems, co-existence of tonic spiking and bursting corresponds to the co-existence of two distinct attractors in the phase space of the system (Fig. 1). Here, we describe bifurcations of a saddle periodic orbit with homoclinic trajectories, which explain this phenomenon. We present a mechanism for this type of bi-stability in a general slow–fast 3D system, as well as provide a qualitative understanding for how either attractor can be observed by varying initial conditions. Our analysis also explains a smooth transition between the regimes. Furthermore, through the analysis, we identify a physiologically plausible parameter that can control the duration of the burst phase and the number of spikes in a burst. We introduce a prototype dynamical system with bifurcation features essential for the phenomenon of bi-stability of tonic spiking and bursting. The bifurcations in our biophysically realistic model are analogous to those in a generic slow–fast 3D system of ODEs written in the form

$$\dot{x} = F(x, z, \alpha), \quad \dot{z} = \mu(g(x, \alpha) - z), \quad (1)$$

where  $x \in R^2$  and  $z$  are phase space variables,  $\alpha$  is a vector of control parameters, and  $0 < \mu \ll 1$ . At  $\mu = 0$ , the *fast* subsystem described by the first equation decouples from the second *slow* one. In this case, the slow variable  $z$  becomes a parameter in the fast subsystem. As for the function  $F$ , its essential properties are illustrated in Fig. 2. First, it ensures that the fast subsystem has either one or three equilibrium states, depending on  $z$ . The branch  $M_{\text{eq}}$  of the equilibria curve for the fast subsystem has a distinctive Z-shape in its projection onto the  $(z, x)$ -phase plane. Its equation is given by  $F(x, z, \alpha) = 0$ . The two turning points of  $M_{\text{eq}}$ , at  $z_{\text{sn}}$  and  $z_{\text{sn}}^*$ , correspond to the saddle-node bifurcations in the fast subsystem where two equilibrium states coalesce forming a double one. Thus the fast subsystem has three equilibria within the interval  $z_{\text{sn}} < z < z_{\text{sn}}^*$ . The middle branch of  $M_{\text{eq}}$  is comprised of saddle points. The upper branch of  $M_{\text{eq}}$ , when stable, corresponds to a depolarized state of the model, whereas the lower one corresponds to a hyperpolarized state. The stable

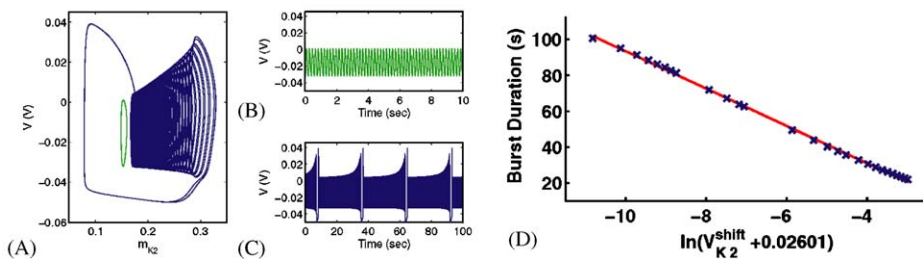


Fig. 1. Co-existence of spiking and bursting modes in the model in the  $(V, m_{K2})$ -projection at the control parameter  $V_{K2}^{\text{shift}} = -0.02598$  V. The small round periodic orbit in A corresponds to the tonic-spikes shown in B; the larger complex orbit in A corresponds to the bursting cycle shown in C. The topology of this bursting cycle (B) is illustrated in Fig. 2. (D) The burst period increases as  $\sim |\ln(V_{K2}^{\text{shift}} + 0.2600866)|$ . Logarithmic fit of the dependence of the burst duration on the control parameter  $V_{K2}^{\text{shift}}$ . Note that the burst duration obeys the same law because the interburst interval hardly changes within the indicated parameter interval. Here,  $V_{K2}^{\text{shift}} = -0.2600866$  is the transition value between the only tonic spiking regime and bi-stability.

focus on the upper branch  $M_{eq}$  is supposed to become unstable, for example, through the supercritical Andronov–Hopf bifurcation at  $z = z_{AH}$ . This means that the stability of the upper branch of  $M_{eq}$  will be imparted, as  $z$  increases, onto the parabolic-like surface  $M_{LC}$  composed of limit cycles of the fast subsystem. As  $z$  increases further, the forthcoming evolution of the stable limit cycle can follow either of two potential scenarios. In the first case, the stable limit cycle is terminated at the homoclinic bifurcation at some  $z_h$  when the saddle point on the middle branch of  $M_{eq}$  has a homoclinic orbit. In addition, the saddle value which is the sum of the two characteristic exponents at the saddle point has to be negative. This means that the stable periodic orbit may merge into the homoclinic loop. In the second case, which is realized in the considered model, a homoclinic bifurcation also occurs, but the saddle value is *positive*. This means that another unstable limit cycle bifurcates from the homoclinic orbit as  $z$  goes through  $z_h$ . As  $z$  grows further, the stable and unstable limit cycles get closer, and they merge into a double limit cycle at some  $z_{sn}^{lc}$ . This is a saddle-node bifurcation for limit cycles in the fast subsystem. After  $z_{sn}^{lc}$  is passed, there exists no limit cycle. This scenario makes the surface  $M_{LC}$  look like as being turned inside out, see Fig. 2. After the stable limit cycle disappears for  $z > z_{sn}^{lc}$ , the phase point moves to another attractor. Such an attractor is a stable equilibrium state on the lower branch of the curve  $M_{eq}$ . If the parameter  $z$  is decreased, the phase point will follow the lower branch towards the saddle-node bifurcation at  $z_{sn}$ . Then the steady-state attractor disappears and the phase point jumps to the stable limit cycle on  $M_{LC}$ . Now that we have described the bifurcation structure of the fast subsystem, let us consider the complete 3D system when  $\mu \neq 0$ . It follows from the work by Fenichel that when  $|\mu| \ll 1$ , the manifold  $M_{eq}$ , whenever it is normally hyperbolic (i.g. far from bifurcations), will persist in the form of some  $\mu$ -close invariant manifold in the singularly perturbed system. Introduce a nullcline  $z = g(x, \alpha)$  on which the  $z$ -variable does not change, i.e.  $\dot{z} = 0$ , see Fig. 2. Below this surface,  $\dot{z}$  is negative, while  $\dot{z} > 0$  on upper branch of  $M_{eq}$  as well as on the surface  $M_{LC}$ . If the above conditions are fulfilled, then the phase point of the 3D system will

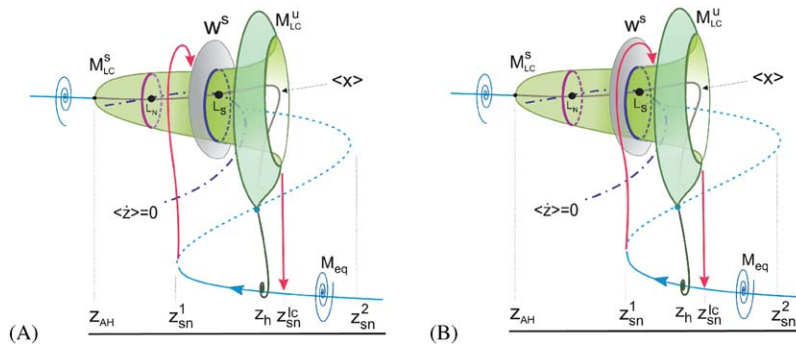


Fig. 2. (A) Points of transverse intersections of  $\langle \dot{z} \rangle = 0$  with  $\langle x \rangle$  are the images of the two periodic orbits: one stable and one saddle in the phase space of the 3D singularly perturbed system. (B) Bi-stability starts when the stable manifold of the saddle periodic orbit bounds the attraction basin of the stable orbit. Transition occurs when the unstable manifold of the saddle periodic orbit becomes homoclinic to the orbit.

behave as follows. It drifts slowly along the lower branch of  $M_{\text{eq}}$  leftward till the fold. Then it makes a rapid jump up on to the perturbed surface  $M_{\text{LC}}$ . Afterwards, it drifts slowly rightward in circular motion around  $M_{\text{LC}}$ . After its  $z$ -component passes through the critical value  $z_{\text{sn}}^{\text{lc}}$ , the phase point falls down on to the lower branch  $M_{\text{eq}}$ , and the cycle starts over again. Such behavior of a trajectory is associated with bursting in neuron models. The number of spikes in a burst is that of complete revolutions around  $M_{\text{LC}}$  between the jump points. A point where the nullcline crosses  $M_{\text{eq}}$  is an equilibrium point in the singularly perturbed system. The coordinates of this point can be found from the condition of the simultaneous vanishing of the right-hand sides of the system (1). We need that nullcline  $\dot{z} = 0$  crosses  $M_{\text{eq}}$  within an unstable interval of  $M_{\text{eq}}$  to avoid stable equilibria in the phase space of the whole system.

Let us first discuss the behavior of the trajectories near the surface  $M_{\text{LC}}$  in the singularly perturbed system. By construction, the outer surface  $M_{\text{LC}}^s$  is spanned by the stable limit cycles of the fast system at  $\mu = 0$ . Define the average value  $\langle x \rangle$  on such a limit cycle  $\varphi(t; z, \alpha)$  over its period  $T$  for a given value of  $z$  as follows:

$$\langle x \rangle = \frac{1}{T(z, \alpha)} \int_0^{T(z, \alpha)} (\varphi(t; z, \alpha), z) dt.$$

By the construction, this curve  $\langle x \rangle$  originates from the Andronov–Hopf bifurcation at  $z_{\text{AH}}$  and terminates at the homoclinic bifurcation at the homoclinic value  $z_{\text{sn}}^{\text{lc}}$  as increases from  $z_{\text{AH}}$ . Note that the curve has a distinctive fold where the stable and unstable limit cycles coalesce (Fig. 2).

It follows from Pontryagin–Rodygin theory [14] that the dynamics of the singularly perturbed system around  $M_{\text{LC}}^s$  is determined by following “averaged” slow subsystem

$$\dot{z} = \frac{\mu}{T(z, \alpha)} \int_0^{T(z, \alpha)} (g(\varphi(t; z), \alpha) - z) dt = \langle G(z, \alpha) \rangle.$$

Hence, if the integral is positive within  $z_{\text{sn}}^{\text{lc}} \leq z \leq z_{\text{sn}}^{\text{lc}}$ , then surface  $M_{\text{LC}}$  is transitive for solutions of the system (1) that coil around  $M_{\text{LC}}$  translating slowly (at the rate of  $\sim \mu$ ) rightward. Such behavior of the system produces the bursting activity. Introduce an average nullcline  $\langle \dot{z} \rangle = 0$  as the parametrically given curve ( $z = \langle g(\zeta) \rangle, x = \langle x(\zeta) \rangle$ ) with

$$\langle g(\zeta) \rangle = \frac{1}{T(\zeta, \alpha)} \int_0^{T(\zeta, \alpha)} g(\varphi(t; \zeta), \alpha) dt$$

and

$$\langle x(\zeta) \rangle = \frac{1}{T(\zeta, \alpha)} \int_0^{T(\zeta, \alpha)} \varphi(t; \zeta, \alpha) dt.$$

Any of its intersection points with the curve  $\langle x \rangle$  corresponds to a zero,  $z^0$ , of  $\langle G \rangle$ , i.e. to a periodic orbit of our system, see Fig. 2. Let there be two such crossing points, i.e. two periodic orbits in the phase space of system (1). The point (periodic orbit) is stable if  $\langle G(z^0, \epsilon) \rangle_z < 0$ , or unstable otherwise. The stability of the periodic orbit in the  $x$ -direction

is determined by that of the corresponding limit cycle  $M_{LC}$  of the fast subsystem at the given  $z^0$ . Therefore, to study bifurcations of stable periodic orbits of the singularly perturbed system, we need to examine the upper branch of the curve  $\langle x \rangle$  corresponding to the stable component  $M_{LC}^s$ . Thus, by construction, one periodic orbit is stable, while the second one is of saddle type because of its instability in the  $z$ -direction.

Here, a very special interest is an interplay between the stable manifold of the saddle periodic orbit that is shown as a grey disk in this figure and the way the phase point jumps up at  $\sim z_{sn}$  (the left fold on the Z-shape curve of equilibria of the fast subsystem) on to the surface  $M_{LC}$ . Two robust situations are possible here. The first shown in Fig. 2(a) is when the phase point gets, once or after some intermediate phase, into the attraction basin of the stable periodic orbit. The system will generate tonic spikes. In the second case illustrated in Fig. 2(b), the stable manifold of the saddle cycle does separate the attraction basin of the stable periodic orbit. This corresponds to the bi-stability in the system, where the tonic-spike solution co-exists with the bursting solution, see the numerical results presented in Fig. 1(a). The choice of the regime is determined by the initial conditions.

When the parameter  $V_{K2}^{shift}$  is decreased, the unstable manifold of the saddle orbit can no longer bound the attraction basin of the stable orbit where the phase point tends to as it jumps off the hyperpolarized phase of the bursting. Observe that the duration of bursting phase may grow with no bound as the control parameter is moved toward the transition value between the regimes, while the interburst interval remains nearly constant. The estimate for the growth of the burst period is given by  $T(z, \alpha^*) |\ln(\alpha - \alpha^*)|$  [19], where  $\alpha^*$  is a deviation of a control parameter from the transition value between the regimes and  $T(z, \alpha^*)$  is the period of the limit cycle on the surface  $M_{LC}$  of the fast subsystem at the given  $z$ . Also note that the bursting behavior is not necessarily regular here but can be chaotic as well, especially when the phase point may pass close by the stable periodic orbit.

We have described a mechanism governing transitions between tonic spiking and bursting regimes. It is based on homoclinic bifurcations of a saddle periodic orbit. This mechanism explains two qualitatively different situations. First, tonic spiking and bursting regimes co-exist and are separated by the saddle periodic orbit. Either regime can be attained by appropriate choice of initial conditions. Second, only tonic spiking is the attracting regime. Also, we studied how the major temporal characteristics of the bursting mode are changing along with the changes of the bifurcation parameter. As a bifurcation parameter we used  $V_{K2}^{shift}$ , which is the potential of half-activation of the slow persistent potassium current. This parameter controls the dynamics of the slowest current. As the control parameter is decreased the duration of the burst grows logarithmically in accordance with the theory of homoclinic bifurcations. At the same time, the interburst interval remains constant. This mechanism and the geometry of the bifurcation are both quite typical for neuronal models based on the Hodgkin–Huxley formalism.

A.S. acknowledges the RFBR Grants nos. 02-01-00273 and 01-01-00975. G.C. and R.L.C. were supported by NIH Grants NS43098. A.S and G.C. appreciate a GSU internal research team grant.

## Appendix

The model studied here is given by

$$CV' = -(\bar{g}_{K2}m_{K2}^2(V - E_K) + g_1(V - E_1) + \bar{g}_{Na}f(-150, 0.0305, V)^3h_{Na}(V - E_{Na})),$$

$$m'_{K2} = [f(-83, 0.018 + V_{K2}^{shift}, V) - m_{K2}]/\tau_{K2},$$

$$h'_{Na} = [f(500, 0.03391, V) - h_{Na}]/\tau_{Na},$$

where the variables  $V$ ,  $m_{K2}$ , and  $h_{Na}$  are the membrane potential, activation of  $I_{K2}$  and inactivation of  $I_{Na}$ , respectively;  $f(x, y, z) = 1/(1 + e^{x(y+z)})$ . The parameters are:  $C = 0.5$  nF is the membrane capacitance,  $\bar{g}_{K2} = 30$  nS is the maximum conductance of  $I_{K2}$ ;  $E_K = -0.07$  V and  $E_{Na} = 0.045$  V are the reversal potentials of  $K^+$  and  $Na^+$ , respectively;  $\bar{g}_{Na} = 200$  nS is the maximal conductance of  $I_{Na}$ ;  $g_1 = 8$  nS and  $E_1 = -0.046$  V are the conductance and reversal potential of the leak current, respectively;  $\tau_{K2} = 0.9$  s and  $\tau_{Na} = 0.0405$  s are the time constants of activation of  $I_{K2}$  and inactivation of  $I_{Na}$ , respectively;  $V_{K2}^{shift}$ , which is the shift of the membrane potential of half-activation of  $I_{K2}$  from its canonical value, is a bifurcation parameter in this study.

## References

- [1] J. Angstadt, W. Friesen, *J. Neurophysiol.* 66 (1991) 1858.
- [2] R. Bertram, *Biol. Cybern.* 69 (1993) 257.
- [3] C.C. Canavier, D.A. Baxter, L. Clark, J. Byrne, *J. Neurophysiol.* 69 (1993) 2252.
- [4] G.S. Cymbalyuk, R.L. Calabrese, *Neurocomputing* 159 (2001).
- [5] G.S. Cymbalyuk, Q. Gaudry, M.A. Masino, R.L. Calabrese, *J. Neurosci.* 22 (2002) 10580.
- [6] A. Hill, J. Lu, M. Masino, O. Olsen, R.L. Calabrese, *J. Comput. Neurosci.* 10 (2001) 281.
- [7] J. Hounsgaard, O. Kiehn, *J. Physiol.* 414 (1989) 265.
- [8] H. Lechner, D. Baxter, C. Clark, J. Byrne, *J. Neurophysiol.* 75 (1996) 957.
- [9] J. Lisman, *Trends Neurosci.* 20 (1997) 38.
- [10] V. Lukaynov, L. Shilnikov, *Soviet Math. Dokl.* 19 (6) (1978) 1314.
- [11] E. Marder, L. Abbott, G. Turrigiano, Z. Liu, J. Golowasch, *Proc. Nat. Acad. Sci. U.S.A.* 26–93 (24) (1996) 13481.
- [12] E. Marder, R.L. Calabrese, *Physiol. Rev.* 76 (1996) 687.
- [13] C.A. Opdyke, R.L. Calabrese, *J. Comput. Physiol.* 175 (1994) 781.
- [14] L.S. Pontryagin, L.V. Rodygin, *Soviet Math. Dokl.* 1 (1960) 611.
- [15] J. Rinzel, *Lecture Notes Math.* 1151 (1985) 304.
- [16] A. Shilnikov, R.L. Calabrese, G. Cymbalyuk, *Phys. Rev. E* (2004), submitted for publication.
- [17] A. Shilnikov, G. Cymbalyuk, *Phys. Rev. Lett.* (2004), in press.
- [18] A. Shilnikov, L. Shilnikov, D. Turaev, *AMS Moscow Math. J.* 4 (2004).
- [19] L. Shilnikov, A. Shilnikov, D. Turaev, L. Chua, in: *Methods Qualitative Theory in Nonlinear Dynamics*, vols. I and II, World Scientific, Singapore, 1998, 2001.
- [20] M. Steriade, D.A. McCormick, T.J. Sejnowski, *Science* 262 (1993) 679.
- [21] D. Terman, *J. Nonlinear Sci.* 2 (1992) 135.
- [22] G. Turrigiano, E. Marder, L. Abbott, *J. Neurophysiol.* 75 (1996) 963.
- [23] X.J. Wang, *Physica D* 62 (1993) 263.